NASA TECHNICAL MEMORANDUM

NASA TM X-3097

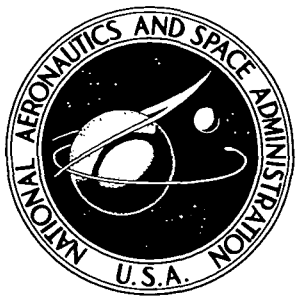

NASA TM X-3097

ON THERMAL STRESS FAILURE OF THE SNAP-19A RTG HEAT SHIELD

by William C. Pitts and Lewis A. Anderson

Ames Research Center
Moffett Field, Calif. 94035

NATIONAL AERONAUTICS AND SPACE ADMINISTRATION • WASHINGTON, D. C. • JULY 1974

1. Report No.	2. Government Accession No.	3. Recipient's Catalog No.
TM X-3097		

4. Title and Subtitle	5. Report Date
ON THERMAL STRESS FAILURE OF THE SNAP-19A RTG HEAT SHIELD	JULY 1974
	6. Performing Organization Code

7. Author(s)	8. Performing Organization Report No.
William C. Pitts and Lewis A. Anderson	A-5516
	10. Work Unit No. 502-19-31
9. Performing Organization Name and Address NASA Ames Research Center Moffett Field, Calif., 94035	11. Contract or Grant No.
	13. Type of Report and Period Covered Technical Memorandum
12. Sponsoring Agency Name and Address National Aeronautics and Space Administration Washington, D. C. 20546	14. Sponsoring Agency Code

15. Supplementary Notes

16. Abstract

Results are presented of a study pertaining to thermal stress problems in an amorphous graphite heat shield that is part of the launch-abort protect system for the SNAP-19A Radioisotope Thermoelectric Generators (RTG) that will be used on the Viking Mars Lander. The first result is from a thermal stress analysis of a full-scale RTG heat source that failed to survive a suborbital entry flight test, possibly due to thermal stress failure. It was calculated that the maximum stress in the heat shield was only 50 percent of the ultimate strength of the material. To provide information on the stress failure criterion used for this calculation, some heat-shield specimens were fractured under abort entry conditions in a plasma arc facility. It was found that in regions free of stress concentrations the POCO graphite heat-shield material did fracture when the local stress reached the ultimate uniaxial stress of the material.

17. Key Words (Suggested by Author(s))	18. Distribution Statement
Thermal shock Thermal stress Failure Criterion SNAP-19A Graphite Stress analysis	Unclassified-Unlimited CAT .32

19. Security Classif. (of this report)	20. Security Classif. (of this page)	21. No. of Pages	22. Price*
Unclassified	Unclassified	10	$3.00

*For sale by the National Technical Information Service, Springfield, Virginia 22151

ON THERMAL STRESS FAILURE OF THE SNAP-19A RTG HEAT SHIELD

William C. Pitts and Lewis A. Anderson

Ames Research Center

SUMMARY

Results are presented of a study pertaining to thermal stress problems in an amorphous graphite heat shield that is part of the launch-abort protect system for the SNAP-19A Radioisotope Thermoelectric Generators (RTG) that will be used on the Viking Mars Lander. The first result is from a thermal stress analysis of a full-scale RTG heat source that failed to survive a suborbital entry flight test, possibly due to thermal stress failure. It was calculated that the maximum stress in the heat shield was only 50 percent of the ultimate strength of the material. To provide information on the stress failure criterion used for this calculation, some heat-shield specimens were fractured under abort entry conditions in a plasma arc facility. It was found that in regions free of stress concentrations the POCO graphite heat-shield material did fracture when the local stress reached the ultimate uniaxial stress of the material.

INTRODUCTION

There are certain space missions for which nuclear energy is the only feasible source of electrical power. For example, the Pioneer-Jupiter missions traveled so far from the Sun that solar energy was precluded as a possible source of electrical power, and the duration of the mission was too great for the use of batteries or fuel cells. Consequently, Radioisotope Thermoelectric Generators (RTG) were chosen as the sole source of electrical power. RTGs were also chosen as the electrical power source for the Viking Mars Lander because they were deemed less vulnerable to the unknown meteorological conditions on the Martian surface.

The use of a nuclear power source in space presents a serious potential hazard in that an early mission abort could disseminate radioactive material into the Earth atmosphere. The current philosophy among engineers concerned with space nuclear safety is to avoid this possibility by enclosing the heat source, which contains the nuclear material, in a protective container called the heat shield. The shield must be able to survive blast pressure, fragment impact, fuel fires, and the high heating rates and temperature encountered during atmospheric entry after an abort. These heating rates can be very high because there is no way to control the velocity or the steepness of descent after an abortion.

The container, therefore, must be made of an ablative, refractory material, which also must be sufficiently heat conductive to allow normal RTG operation. POCO graphite meets these requirements and has been selected as the heat-shield material for the SNAP-19 RTG. Carbon phenolic or elastomeric materials, which have advantages for the lower temperature environment of controlled atmospheric entry, cannot survive the high temperatures. It was shown in reference 1 that a POCO graphite heat shield for the SNAP-19 RTG heat source can safely contain the fuel until Earth impact for the reentry conditions after a Nimbus B abort.

In an evaluation of the suitability of a material for the heat shield, one of the most crucial factors for aborted missions is the ability of the material to withstand thermal shock. Much work was done to assess the ability of POCO graphite to withstand thermal shock as the heat-shield material of the SNAP-19 RTGs for the Pioneer-Jupiter missions (ref. 2). In reference 2 it was shown by numerical calculations that a POCO graphite heat shield could survive most of the expected conditions for entry after abort for this mission, but for some combinations of high velocity and steep descent, cracks were predicted to form on the inner surface of the heat shield because of excessive thermal stress.

The question was raised, but not answered, about whether these cracks would propagate to cause a catastrophic failure of the heat shield. Another unknown factor was the value of the stress concentration factor to be used for the threads at the ends of the heat source. A third uncertainty was the criterion to be used to relate the calculated thermal stresses to the condition for material cracking or failure. Because amorphous graphite is a brittle material, the common maximum normal stress criterion for brittle material was used. This criterion states that failure will occur whenever the local normal stress exceeds the uniaxial strength of the material. However, some experts feel that a thermal stress is a "secondary stress," which implies that the stress must exceed the stated criterion before thermal stress failure will occur.

In view of the uncertainties in predicting thermal stress failure conditions and the lack of experimental data, a full-scale SNAP-19 heat source model was placed on the HAVE SINEW-1 test flight along with five other heat source models (ref. 3). During this flight, the six models were released at an altitude of 94 km. Four of the heat sources survived entry and were recovered, but the other two, including the SNAP-19 heat source, were never found. Evidence shows that at least one of the missing heat sources broke up in flight, but the evidence does not show which of the two it was. There is the possibility that the second missing model landed outside the search area, but more likely it too broke up in flight. The reason for failure in flight has not been established but there are several possibilities including improper release from the payload adapter, excessive vibrations, and thermal stress failure. Thermal stress failure is cited in reference 3 as the most likely cause.

This discussion is directed to the question of thermal stress failure of the SNAP-19A RTG heat shield. The SNAP-19A RTG, which is very similar to the SNAP-19 RTG, is to be the electric power source for the Viking Mars Lander.

In the first part of the paper the results of a thermal stress analysis are presented for the SNAP-19 heat source model during its HAVE SINEW-1 flight. Then, the results of an experimental and theoretical analysis are presented for SNAP-19A heat shields that were thermally fractured in a plasma jet that simulated flight abort conditions.

GENERAL ANALYSIS PROCEDURE

The finite-element model used for thermal analysis is shown in figure 1. It is a two-dimensional cross section of the heat source of the SNAP-19A RTG

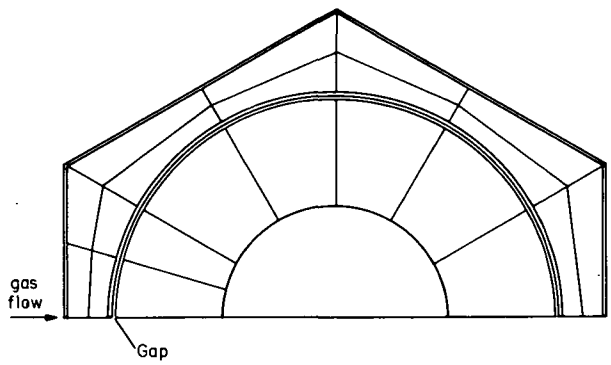

Figure 1.- Finite-element model used in CINDA thermal analysis.

shown in figure 2. Due to symmetry, only half of the model need be considered. The portion outside the gap is the abort reentry heat shield made of POCO graphite AXF-Q1. The inner portion will be either the Pioneer heat source configuration or a graphite cylinder. The validity of using this two-dimensional model to analyze the Pioneer heat source is discussed in reference 2, where it is concluded that good accuracy will be obtained for the center sections of the Pioneer heat source if the two-dimensional model is used. There will be some error near the ends of the heat source, but this will be small compared to the uncertainty created by the stress concentration due to the threads (fig. 2). Because analysis of these stress concentrations was beyond the scope of this study, the two-dimensional model was deemed adequate for present purposes.

The thermal analysis for this study was performed using the CINDA-3G code (Chrysler Improved Numerical Differencing Analyzer for 3rd Generation Computers, ref. 4). CINDA is a general code that has great flexibility and can handle problems of nearly unlimited complexity. For the present problem, the program accounts for aerodynamic heating, ablation, subsonic convection, radiation, and conduction, all in the manner described in references 2 and 5. The procedures for providing the aerodynamic heating input are discussed later in connection with specific problems.

The two-dimensional, finite-element model used for the stress analysis is similar to that used for the thermal analysis except that only the reentry

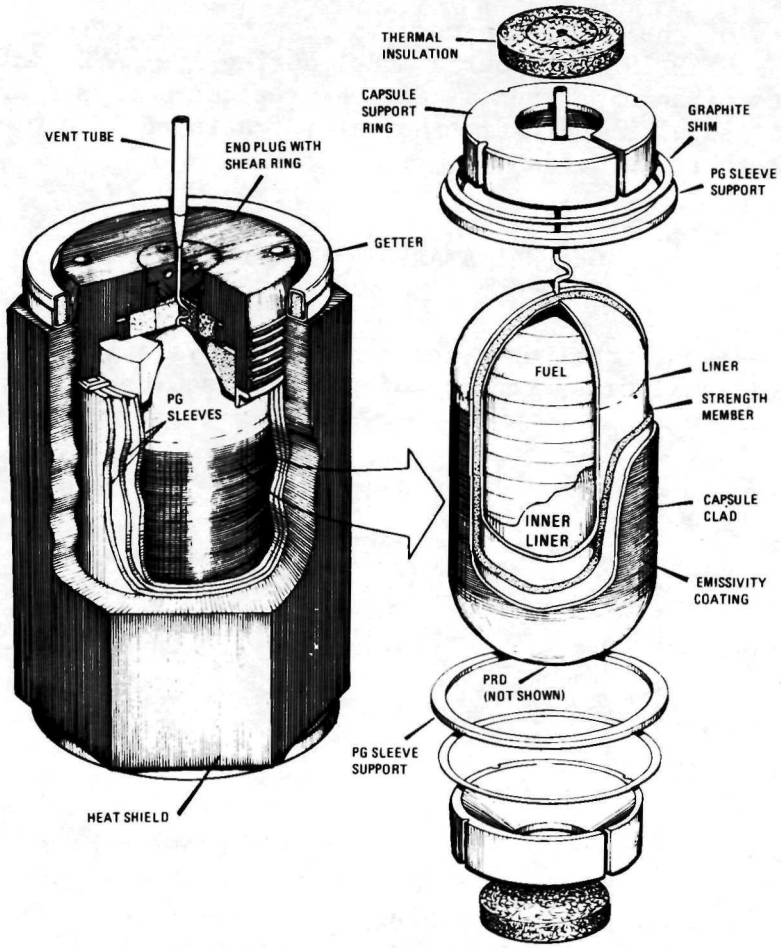

Figure 2.- SNAP-19A heat source.

heat shield is considered and the element size is much smaller. The front portion (flow stagnation region) of this model is shown in figure 3. The remainder of the model is made up of rectangular elements about the size of those on the right side of the figure.

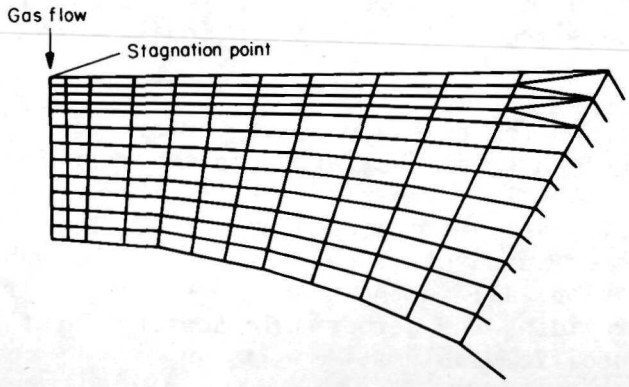

Figure 3.- Finite-element model used in NASTRAN stress analysis.

The stress analysis for this model was performed using the NASTRAN finite-element program (ref. 6). The model temperature distributions obtained from the CINDA thermal stress analysis were used as input to the NASTRAN program to calculate the thermal stresses. Aerodynamic pressure forces and, where applicable, inertial forces were also included in the stress analysis, but these forces were found to produce negligible stresses compared to the thermal stresses.

HAVE SINEW-1 STRESSES

As stated in the Introduction and in reference 3, two of the HAVE SINEW-1 models were not recovered, possibly because they broke up due to thermal stress failure. A preliminary test had indicated that thermal failure was not likely, but no quantitative stress analyses had been made. A two-dimensional stress analysis has now been made using the models shown in figures 1 and 3; results are shown in figure 4. The maximum stresses occur near the stagnation region, so only the stress pattern in that region of the model is shown. Lines of constant stress ratio (local stress/ultimate stress at local temperature) are superimposed on the model profile. The stress is compressive near the front and tensile near the inner portion of the model, but nowhere does it exceed 50 percent of the ultimate stress of the material. Thus, if a stress ratio of 1.0 is a valid criterion for failure, thermal stress failure is not predicted in the midsection of the heat source. However, failure is possible near the ends where the threads cause stress concentrations. For failure to occur, either the stress concentration factor at the ends must be the order of 2 or the stress ratio is not a proper failure criterion. The latter possibility is discussed further in the remainder of the paper.

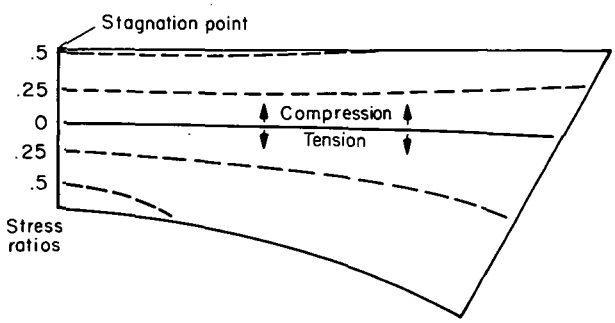

Figure 4.- Lines of constant stress ratio (local stress/ultimate stress at local temperature) for two-dimensional portion of HAVE SINEW-1 model.

THERMAL STRESS TEST

To examine the thermal stress fracture criterion several sections of POCO AXF-Q1 graphite were thermally fractured in the Ames 6-cm Plasma Arc. A typical specimen assembly is shown in figure 5. The hexagonal cross section of the specimen is that of a full-size replica of the reentry heat shield of a SNAP-19A heat source (figs. 1 and 2). It is 8.9 cm across the flats. Two of the sections are 1 cm wide and the other is 2 cm wide. These three sections are supported at the ends by solid hexagonal cylinders of graphite and in the center by a thick circular cylinder of graphite. Four wire spacers form the

0.15-cm gap shown in figure 1. This entire assembly is mounted on a stainless-steel tube, which is used to support the model in the plasma arc facility.

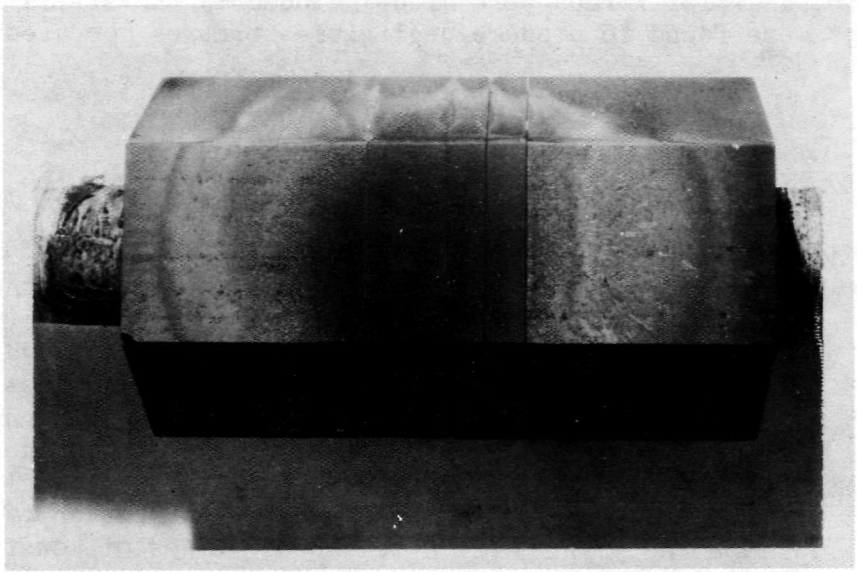

Figure 5.- Model assembly after run showing crack pattern and extent of plasma coverage.

The assembly shown in figure 5 was subjected to a stagnation cold wall heating rate of about 8 kw/cm^2 for 0.89 sec. Nitrogen gas was used in the arc to avoid oxidation of the graphite. The size of the plasma jet can be seen from the ring pattern on the face of the specimen assembly. The enthalpy is not uniform across the entire jet, but it is reasonably uniform within the black spot region in figure 5. The specimen temperature was monitored at two points during the run. The inside surface temperature was measured with a thermocouple cemented to the inner surface, and the stagnation point temperature was measured with an optical pyrometer that viewed in the 8000 to 8050 Å wavelength range. For this range, the plasma stream is transparent.

Two of the three specimens (fig. 5) cracked during the test. These cracks are shown in figure 6, which is a closeup of figure 5. The crack in the 2-cm-wide specimen penetrated the entire depth of the specimen; the crack in the 1-cm specimen, however, stopped about 0.1 cm from the inner surface, as shown in figure 7. The straight line behind the inner surface is a 0.075-cm-diam wire placed there for size comparison purposes.

A total of four heat-shield sections were run under similar conditions. In addition to the three sections shown in figure 5, a 4-cm wide specimen was run. It did not crack. The fact that some but not all the specimens cracked suggests that the test conditions produced threshold thermal stresses for fracture; actual fracture depended on the variation of material properties among specimens.

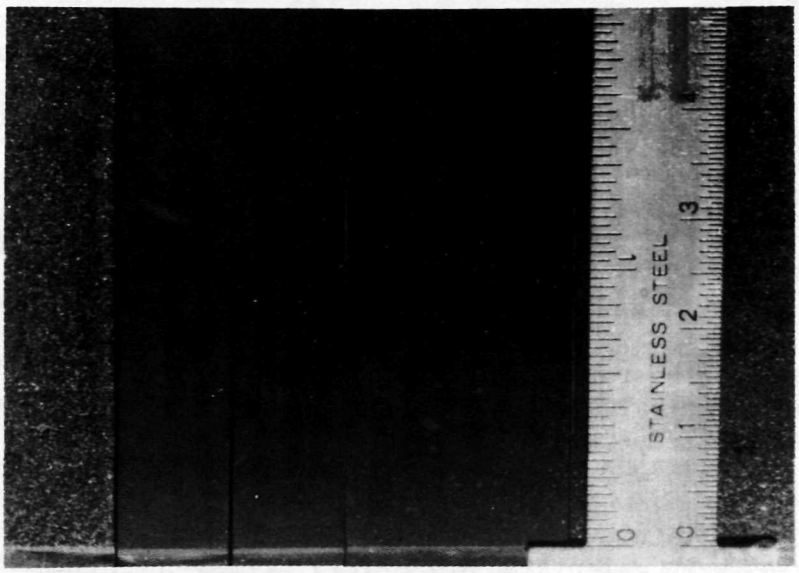

Figure 6.- Closeup of cracks from front view, figure 5.

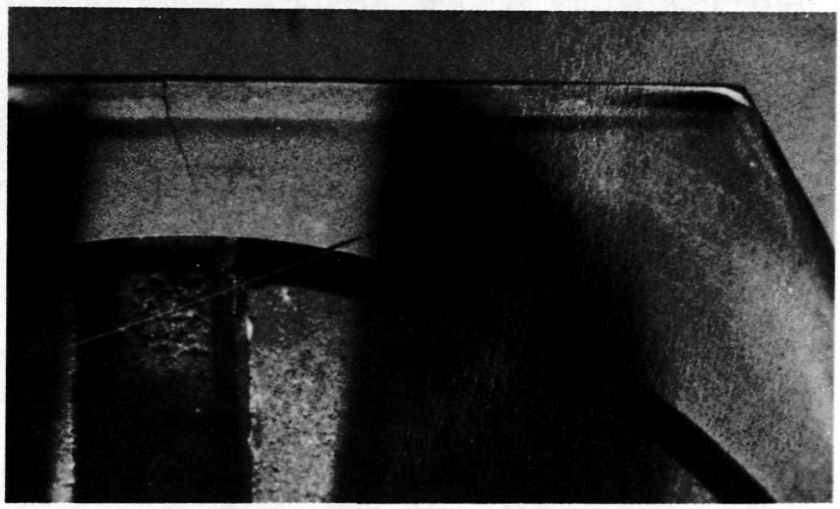

Figure 7.- Side view of crack in 1-cm-thick specimen.

THERMAL STRESS ANALYSIS

A thermal stress analysis for the specimen in figure 7 was made to determine the stress ratio in the material at the crack site. Because only an approximate, average value of the model heating rate was measured, the first step in the analysis was to determine a better value for this quantity as a function of time. This was done by trial-and-error tailoring of the approximate heating rate until the temperature calculated using CINDA agreed with the measured values at the stagnation point and inner surface of the specimen for the full time of the run. The resulting heating rate variation

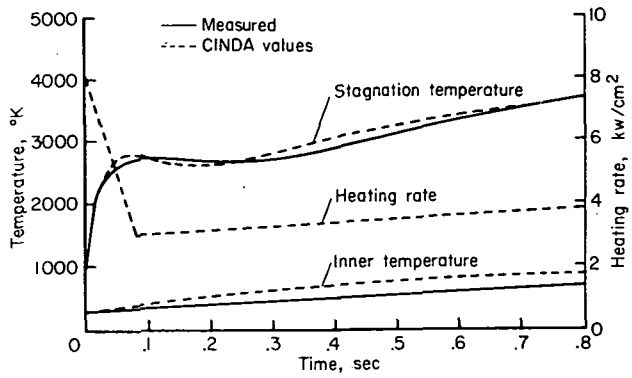

Figure 8.- Temperature history match between measured and calculated values of specimen temperatures.

with time is shown in figure 8, together with the temperatures calculated using this heating rate. The measured temperatures are also shown. The calculated stagnation temperature is quite sensitive to the choice of heating rate. The fact that the calculated inner surface temperature is higher than the measured value is reasonable both because the mounting cement for the thermocouple restricted heat transfer to the junction and the lead wires conducted heat away from the junction.

The heat-shield stresses were then calculated using the NASTRAN program with the temperature output from CINDA and the finite-element model of figure 3. Stresses were calculated for several times during the test run, and the maximum stress was found to occur on a rather flat maximum between 0.05 and 0.07 sec into the run, which corresponds to the time of the first peak in stagnation temperature in figure 8. The calculated temperature distribution is shown in figure 9 at $t = 0.06$ sec. The stress field for that same time is presented in figure 10 in the stress-ratio form. The normalizing stress is the average ultimate stress for POCO AXF-Q1 at the local specimen temperature.

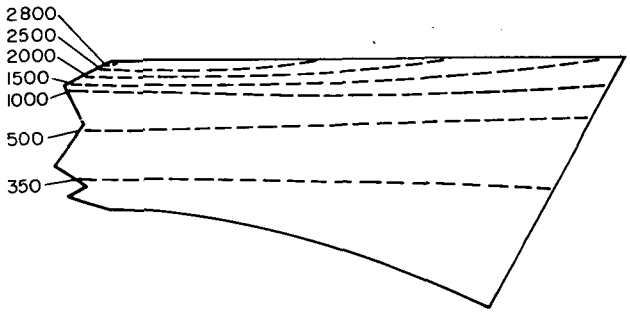

Figure 9.- Calculated temperature profiles in specimen at $t = 0.06$ sec, °K.

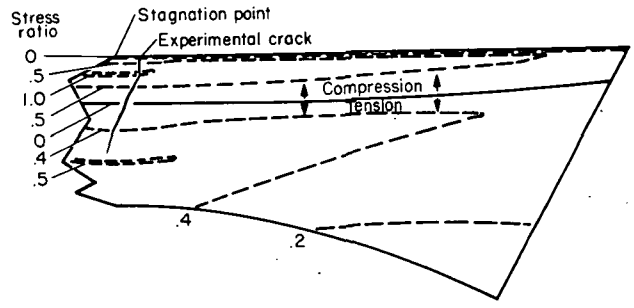

Figure 10.- Crack and calculated stress contours in specimen at time of maximum thermal stress, $t = 0.06$ sec.

The crack that formed in the specimen (fig. 7) is superimposed on the calculated stress field. The stress shown is the principal stress with maximum magnitude. The axis of this principal stress is within 2° of being normal to the front surface. The stress parallel to the front surface is nearly zero everywhere so that the stress field is essentially uniaxial. The stress normal to the front surface is zero as required by boundary conditions because a surface cannot support a stress perpendicular to itself. The stress ratio rises rapidly behind the stagnation point to a value of 1.0 for a small distance from the centerline.

Interestingly, the experimentally observed crack passes through the stress ratio equal to 1.0 line. In all probability, the crack initiated near

this intersection because in the tension region the maximum local stress is only 50 percent of the ultimate stress of POCO. It might not be expected a priori that a crack would initiate in a region of compressive stress, but it is possible. If a crack is located in a region of uniaxial compression, as in figure 11, the shearing force along the crack can cause large tensile stresses along the crack surface near its tip. In reference 7, Hoek and Bieniawski discuss in detail the conditions for propagation of a small crack under a compressive load. They conclude that the only way that a crack can propagate to the point of specimen failure under a purely compressive load is if the loading is uniaxial. They also conclude that the crack will form parallel to the compressive stress direction. Both of these conditions prevail in the present example.

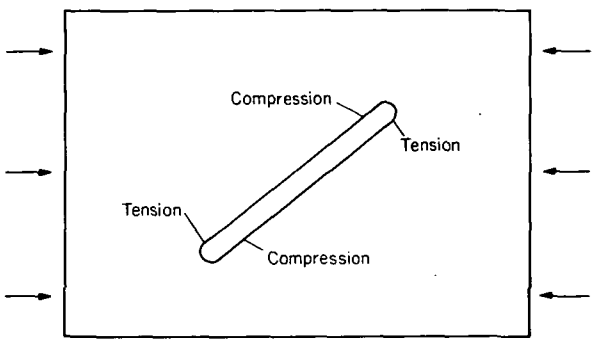

Figure 11.- Form of stress variation around crack in plate under uniaxial compression.

Because the maximum stress ratio calculated for the specimens of this study is 1.0, the conditions of the experiment are predicted to be marginal for failure, if the stress ratio is a proper stress failure criterion. That the test conditions were threshold values for thermal failure was also indicated by the experimental data. Of the four specimen run under similar conditions, two cracked during the run and two survived. For the other specimen that failed, the crack was very similar in form and location to the one discussed above, except that it continued to the inner surface, completely severing the specimen.

CONCLUSIONS

The SNAP-19 (Pioneer/Viking) RTG heat source model was lost during the HAVE SINEW-1 flight, possibly due to thermal stress failure of the heat shield. A thermal stress calculation was made for this model for the conditions experienced in the HAVE SINEW-1 flight, and it was found that the maximum thermal stresses were only about half the ultimate thermal stress capability of the heat-shield material, POCO AXF-Q1. Therefore, for thermal stress failure to have occurred, either the stress concentration factor for the end threads must be the order of 2, or the stress failure criterion used was not correct.

The stress failure criterion was examined as the second part of this study. Sections of a full-scale SNAP-19A heat shield were subjected to a reentry type environment. Under essentially the same conditions two of the specimens failed and two survived, which indicated a threshold condition existed for thermal stress failure. A thermal stress analysis of the model for the test conditions also indicated a marginal condition for failure because the local stress was equal to the ultimate stress of the material in

the vicinity of the crack. Thus, for POCO graphite at least, a value of 1.0 for the ratio of local stress to ultimate stress seems to be a reasonable stress criterion when there are no stress concentrations due to irregularities such as threads or holes.

Ames Research Center
National Aeronautics and Space Administration
Moffett Field, Calif. 94035, May 21, 1974

REFERENCES

1. Klett, R. D.: *Thermal Design of a SNAP-19 Generator for Intact Reentry.* Sandia Laboratories, SC-RR-67-197, 1967.

2. Stewart, R.E.D.: Pioneer Heat Source Aerothermodynamic Analysis: Vol. V - Thermal Stress Analysis. Sandia Laboratories, SC-RR-71-0168, 1971.

3. Bustamante, A. C.; Randall, D. E.; and McAlees, S.: HAVE SINEW-1 Post-flight Report. Sandia Laboratories, SC-RR-72-0225, 1972.

4. Lewis, R. D.; Gaski, J. D.; and Thompson, L. R.: Chrysler Improved Numerical Differencing Analyzer for Third Generation Computers. Chrysler Corporation, Space Division, New Orleans, La., TN-AP-67-287, 1967.

5. Klett, R. D.: Pioneer Heat Source Aerothermodynamic Analysis: Vol. 3 - Aeroheating, Ablation and Design Modifications. Sandia Laboratories, SC-RR-71 0168, 1971.

6. Butler, Thomas G.; and Michel, Douglas: NASTRAN-A Summary of the Functions and Capabilities of the NASA Structural Analysis Computer System. NASA SP-260, 1971.

7. Hoek, E.; and Bieniawski, Z. T.: Brittle Fracture Propagation in Rock Under Compression. Intl. Jour. of Fracture Mechanics, vol. 1, no. 3, Sept. 1965, pp. 137-155.

NATIONAL AERONAUTICS AND SPACE ADMINISTRATION
WASHINGTON, D.C. 20546

OFFICIAL BUSINESS
PENALTY FOR PRIVATE USE $300

SPECIAL FOURTH-CLASS RATE
BOOK

POSTAGE AND FEES PAID
NATIONAL AERONAUTICS AND
SPACE ADMINISTRATION
451

U.S.MAIL

POSTMASTER: If Undeliverable (Section 158 Postal Manual) Do Not Return

"The aeronautical and space activities of the United States shall be conducted so as to contribute . . . to the expansion of human knowledge of phenomena in the atmosphere and space. The Administration shall provide for the widest practicable and appropriate dissemination of information concerning its activities and the results thereof."

—NATIONAL AERONAUTICS AND SPACE ACT OF 1958

NASA SCIENTIFIC AND TECHNICAL PUBLICATIONS

TECHNICAL REPORTS: Scientific and technical information considered important, complete, and a lasting contribution to existing knowledge.

TECHNICAL NOTES: Information less broad in scope but nevertheless of importance as a contribution to existing knowledge.

TECHNICAL MEMORANDUMS: Information receiving limited distribution because of preliminary data, security classification, or other reasons. Also includes conference proceedings with either limited or unlimited distribution.

CONTRACTOR REPORTS: Scientific and technical information generated under a NASA contract or grant and considered an important contribution to existing knowledge.

TECHNICAL TRANSLATIONS: Information published in a foreign language considered to merit NASA distribution in English.

SPECIAL PUBLICATIONS: Information derived from or of value to NASA activities. Publications include final reports of major projects, monographs, data compilations, handbooks, sourcebooks, and special bibliographies.

TECHNOLOGY UTILIZATION PUBLICATIONS: Information on technology used by NASA that may be of particular interest in commercial and other non-aerospace applications. Publications include Tech Briefs, Technology Utilization Reports and Technology Surveys.

Details on the availability of these publications may be obtained from:

SCIENTIFIC AND TECHNICAL INFORMATION OFFICE

NATIONAL AERONAUTICS AND SPACE ADMINISTRATION

Washington, D.C. 20546